

Structural analysis of the yeast SWI/SNF chromatin remodeling complex

Corey L. Smith¹, Rachel Horowitz-Scherer², Joan F. Flanagan¹, Christopher L. Woodcock² and Craig L. Peterson¹

Published online 13 January 2003; doi:10.1038/nsb888

Elucidating the mechanism of ATP-dependent chromatin remodeling is one of the largest challenges in the field of gene regulation. One of the missing pieces in understanding this process is detailed structural information on the enzymes that catalyze the remodeling reactions. Here we use a combination of subunit radio-iodination and scanning transmission electron microscopy to determine the subunit stoichiometry and native molecular weight of the yeast SWI/SNF complex. We also report a three-dimensional reconstruction of yeast SWI/SNF derived from electron micrographs.

SWI/SNF is a large multisubunit assembly that contains the products of several genes originally identified in *Saccharomyces cerevisiae* by defects in mating type switching (SWI) and/or sucrose fermentation (SNF; sucrose non-fermenting)¹. Yeast SWI/SNF is required for expression of a subset of highly inducible genes, as well as transcription of numerous genes expressed during late mitosis². SWI/SNF is highly conserved in eukaryotes, and SWI/SNF complexes from both *Drosophila* and humans have been implicated in the transcriptional control of numerous genes². SWI/SNF complexes have been purified from yeast, *Drosophila* and humans, and each of these purified complexes use the energy of ATP hydrolysis to enhance the accessibility of nucleosomal DNA³. Although SWI/SNF clearly plays key roles in the regulation of eukaryotic gene expression, the mechanistic basis for how SWI/SNF uses the energy of ATP hydrolysis to alter nucleosome structure still remains a mystery. Here we have addressed this general question by characterizing the subunit stoichiometry, native molecular weight (M_w) and three-dimensional structure of yeast SWI/SNF.

Subunit stoichiometry of yeast SWI/SNF

First, we established the relative stoichiometry of the 11 different SWI/SNF polypeptides. Gel filtration analyses have estimated the native M_w of both the yeast and human SWI/SNF complexes to be ~2 MDa^{4,5}. These previous studies, however, yielded only a rough estimate for the native M_w of SWI/SNF because no protein standards >660 kDa could be included. Analysis of purified SWI/SNF by SDS-PAGE suggests that each subunit is present at 1:1 stoichiometry, with the exception of the Swi3p subunit, which stains more intensely with both silver and Coomassie. However, the summed M_w of the individual subunits of the SWI/SNF complex amount to only ~1 MDa, suggesting that the SWI/SNF complex may contain two copies of each subunit.

As a first step towards understanding the stoichiometry of SWI/SNF subunits, we sought to determine the copy number of the Swi2p/Snf2p ATPase subunit. To this end, we used two different epitope-tagged protein variants of Swi2p to create three different haploid yeast strains. Two control strains carried alleles encoding either a triple HA-tagged SWI2 (SWI2-HA₃) inte-

grated at the *URA3* locus or a Myc₁₈-tagged SWI2 (SWI2-Myc₁₈) integrated at the chromosomal *SWI2* locus. The test strain contained both epitope-tagged proteins. Each epitope-tagged protein variant was expressed from the normal *SWI2* upstream regulatory region, and each epitope-tagged protein was able to complement the phenotypes of a *swi2* deletion allele (data not shown), indicating that they are fully functional *in vivo*.

Whole cell extracts were prepared from each strain, and SWI/SNF was immunoprecipitated using antibodies specific to either the Myc or HA epitopes (Fig. 1). In the case of the control strains, each antisera immunoprecipitated only the expected epitope-tagged Swi2p, confirming the specificity of these sera. In the test strain that contains both tagged alleles, immunoprecipitations with the anti-HA sera precipitated only SWI/SNF complexes harboring the HA₃-tagged Swi2p. Likewise, the anti-Myc sera immunoprecipitated the Myc₁₈-tagged allele of Swi2p,

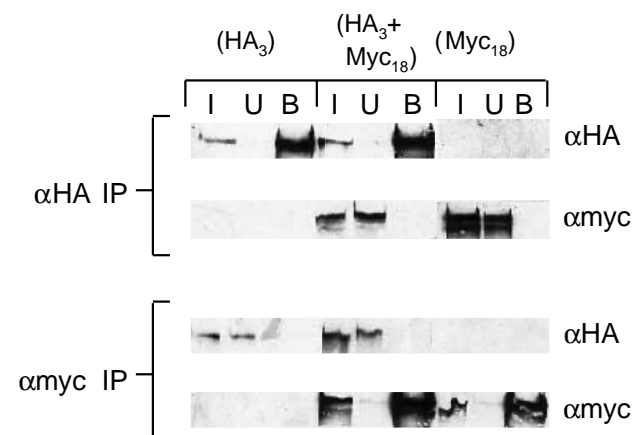


Fig. 1 Swi2p was immunoprecipitated from whole cell extracts made from yeast strains CY831 (SWI2-HA₃), CY832 (SWI2-Myc₁₈) and CY889 (SWI2-Myc₁₈/SWI2-HA₃). Lanes are labeled I, U or B for input (2.5%), unbound (2.5%) or bound (100%), respectively. Immunoprecipitation experiments were performed with either monoclonal anti-HA or anti-Myc immune sera. The presence of Swi2p was detected with either anti-HA or anti-Myc by western blot analysis.

¹University of Massachusetts Medical School, Program in Molecular Medicine, Worcester, Massachusetts 01605, USA. ²University of Massachusetts, Department of Biology, Amherst, Massachusetts 01003, USA.

Correspondence should be addressed to C.L.P. e-mail: Craig.Peterson@umassmed.edu

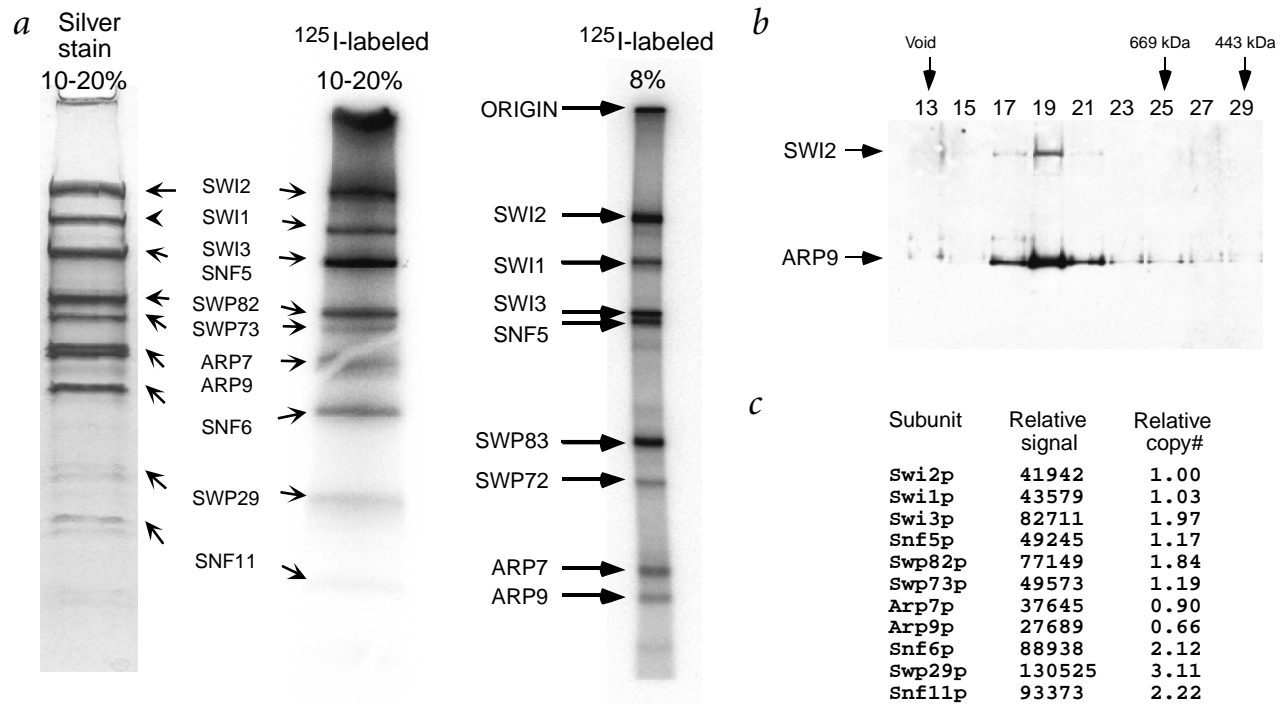


Fig. 2 Purification and stoichiometry of the SWI/SNF complex. Denatured SWI/SNF (5 pmol) was tyrosine-labeled with [¹²⁵I]NaI in the presence of chloramine T. Labeled complex was electrophoresed on SDS-PAGE gels and subjected to analysis by densitometry using a PhosphorImager. Signal intensity was determined per tyrosine in each subunit. Stoichiometry was determined by comparing the tyrosine signal strength of each subunit to that of Swi2p, which is known to be present in just one copy in the complex. **a**, ¹²⁵I-labeled SWI/SNF run on either a 10–20% or 8% SDS-PAGE gel compared with silver stain of same preparation. **b**, Gel filtration analysis of TAP-tagged SWI/SNF. A 100 μl sample of SWI/SNF purified by the TAP protocol was fractionated on a Superose 6 HR10/20 gel filtration column (Pharmacia) as described⁴. The elution positions of protein standards are indicated at the top of the panel. Fractions were assayed for SWI/SNF using western blot analysis and polyclonal antibodies (Santa Cruz Biotechnology) to the Arp9p subunit, which crossreacts with Swi2p. **c**, PhosphorImager quantification of data shown in (a). Relative signal reflects the raw PhosphorImager signal normalized to tyrosine number. Copy number shown is relative to Swi2p. Similar results were obtained from several independent labelings and several different gel separations. Note that the under-representation of Arp9p was not observed in other experiments.

but not the HA-tagged allele of Swi2p. Thus, these results indicate that yeast SWI/SNF contains only one copy of the Swi2p ATPase subunit.

To determine the stoichiometry of the remaining SWI/SNF subunits, we used quantitative tyrosine iodination⁶. In this method, purified SWI/SNF is denatured in SDS, and tyrosine residues are labeled with ¹²⁵I in a chloramine T-oxidation procedure. ¹²⁵I-labeled SWI/SNF complex is then electrophoresed on SDS-PAGE, and iodine incorporation is quantified using PhosphorImager analysis. Because the number of tyrosine residues is known for each SWI/SNF subunit, this method allows determination of the number of copies of each SWI/SNF subunit relative to the known single copy of Swi2p. In preliminary experiments, however, we found that ¹²⁵I-labeling of minor contaminating polypeptides in our SWI/SNF preparations occluded quantification of several SWI/SNF subunits.

To improve the purity of our SWI/SNF preparation, we used a tandem affinity purification (TAP) scheme^{7,8}. We created a yeast strain harboring a SWI2 gene with a TAP module inserted at the C terminus. The SWI2-TAP allele is expressed from its normal chromosomal position and this allele fully complements the phenotypes of a swi2 deletion allele (data not shown). Whole cell

extracts were prepared from this strain, and SWI/SNF complex was purified by sequential affinity purification on IgG-agarose and calmodulin affinity resins. SWI/SNF purified by the TAP protocol was determined to be >90% pure by SDS-PAGE analysis and contained the diagnostic 11 polypeptides detected by silver staining (Fig. 2a). The affinity purified SWI/SNF elutes from a Superose 6 gel filtration column with an apparent M_w of 2 MDa (fraction 19, Fig. 2b)⁴, and the ATPase and nucleosomal array remodeling activities of this complex were identical to that of SWI/SNF purified by standard chromatography⁴ (data not shown).

TAP-purified SWI/SNF was denatured in SDS and quantitatively radio-iodinated on tyrosine residues. Labeled SWI/SNF subunits were separated by SDS-PAGE, and iodine incorporation was

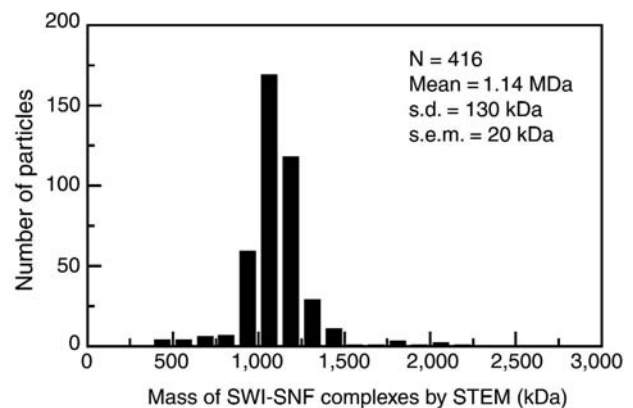
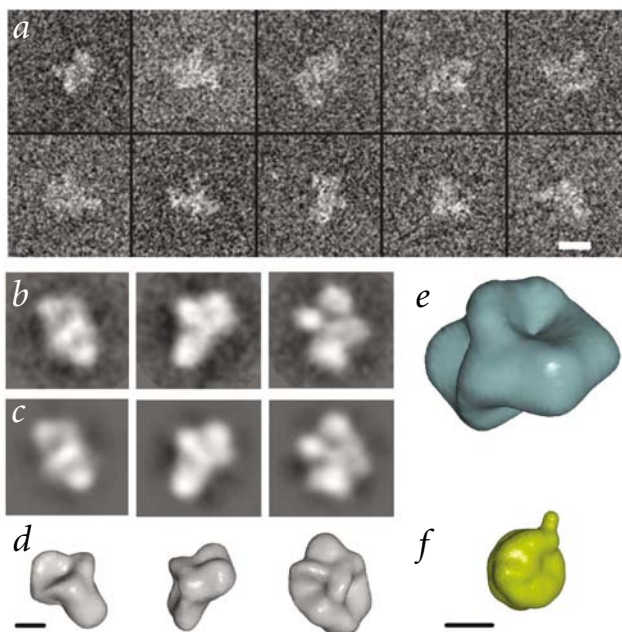


Fig. 3 STEM mass analysis of individual SWI/SNF complexes reveals a unimodal distribution with a mean of 1.14 MDa. TAP-purified SWI/SNF was crosslinked, applied to carbon films, freeze-dried and imaged by STEM. Scattering from individual particles were recorded, and converted to absolute mass. s.d. = standard deviation, and s.e.m. = standard error of the mean.

Fig. 4 3D structure of the yeast SWI/SNF complex. **a**, Raw images. **b**, Examples of class averages identified by EMAN¹¹. **c**, Projections of the final 3D structure at the same angles as the class averages show an excellent match between the two. **d**, Rendered surface of 3D structure viewed at the same angle as the projections. **e**, Rendered surface with the cone-shaped depression at top, filtered to 3.0 nm resolution. **f**, Rendered surface of the nucleosome core particle¹², the SWI/SNF substrate, filtered to the same resolution. The scale bars are 10 nm.



quantified using PhosphorImager analysis (Fig. 2*b,c*). Signal strength per tyrosine residue was determined and compared with the Swi2p signal to determine relative stoichiometry (Fig. 2*c*). The results of the tyrosine iodination indicate that 6 of the 11 subunits are present in single copy (Swi2p, Swi1p, Snf5p, Swp73p, Arp7p and Arp9p). The other five are present in multiple copies (two copies of Swi3p, Swp82p, Snf6p and Snf11p, and three copies of Swp29p). On the basis of this stoichiometry, SWI/SNF is predicted to have an apparent molecular mass of only 1.15 MDa.

STEM mass analysis

As an independent method to determine the native M_w of yeast SWI/SNF, we used scanning transmission electron microscopy (STEM), in which the linear relationship between electron scattering and sample mass provides accurate determinations of M_w up to 10 GDa⁹. TAP-purified SWI/SNF was crosslinked with 0.1% (v/v) glutaraldehyde for 16 h in high salt buffer, the samples were freeze-dried on carbon films and scattering data were recorded (see Methods). SWI/SNF complexes, which appeared as roughly circular particles, were selected, and the mass was determined after correcting for the carbon film background. The histogram (Fig. 3), which includes all particles ($n = 416$) from several images, shows a

unimodal distribution with a mean of 1.14 MDa (standard error ~20 kDa), in excellent agreement with the stoichiometric data.

3D structure of SWI/SNF in negative stain

Although STEM provides accurate mass values, the images are generally less informative about structure, probably because of interactions with the carbon substrate and collapse during freeze-drying⁹. To determine the 3D structure of the complex, we imaged TAP-purified SWI/SNF in neutral sodium phosphotungstate. The raw images indicated an oblate shape ~25 nm by ~12 nm, with several prominent lobes (Fig. 4*a*). This is quite similar to the multi-lobed appearance of human SWI/SNF imaged by atomic force microscopy¹⁰. Single particle reconstruction¹¹ with three separate input data sets of ~5,000–10,000 images, resulted in 3D reconstructions with excellent agreement between class averages and their corresponding angular projections from the final reconstruction (Fig. 4*b–d*). The three independent reconstructions were calculated with data from different isolations of SWI/SNF, each separately prepared for EM. The starting models were generated by reference-free classification, thereby avoiding the types of bias that can result from selection of external starting models. Similar 3D shapes and volumes were derived from all three data sets, pairwise comparisons indicating congruent structures to 3.5–5.0 nm resolution (see Methods; Fig. 4*e*). The data have been low-pass filtered to a resolution of 3.0 nm, and the surface is rendered to enclose a volume corresponding to 1.14 MDa protein. For comparison, a representation of the nucleosome core particle¹² at the same magnification and resolution is shown (Fig. 4*f*). Analysis of the 3D reconstructions revealed distinct mass centers that may provide clues to the locations of the SWI/SNF polypeptides. Centers 1–6 form a ring of lobes that create the rim of a large conical depression

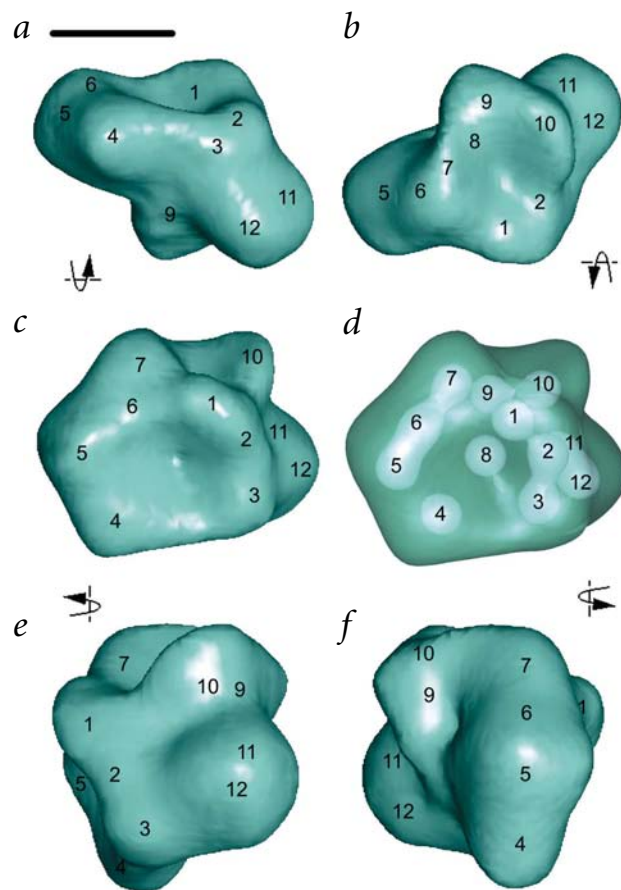


Fig. 5 Principal features of the SWI/SNF reconstruction shown in Fig. 4. The SWI/SNF complexes shown in **a,b**, are 90° rotations about the horizontal plane of **c,d**, the 'front' views, with the surface lobes origination from the individual centers labeled. In **(d)**, the semi-transparent areas show the 12 centers of mass (numbered arbitrarily). Note that there is no corresponding lobe in **(c)** for mass center 8. In the other views, the surface lobes arising from each mass center are labeled. **e,f**, 90° rotations about the vertical plane of **(c,d)**. The rim of the cone-shaped depression is formed from masses 1–6, with 8 near the base. The scale bar is 10 nm.

sion or pocket ~15 nm in diameter and ~5 nm in depth (Fig. 5c,d). The dimensions of this large cavity make it an excellent candidate for a potential nucleosome-binding pocket. Other lobes appear to originate from centers 7 and 9–12 and are more clearly seen from other views of the complex (Fig. 5 a,b,e,f). Mass center 8, which is located beneath the depression, is unique in having no associated surface lobe. A preliminary analysis of SWI/SNF in complex with 200 base pairs of DNA did not reveal a unique DNA-binding site (not shown), suggesting that a single SWI/SNF particle can bind DNA on multiple sites¹³.

This work provides the first characterization of the mass, polypeptide stoichiometry and 3D structure of a low abundance, large multi-subunit chromatin remodeling complex, opening the way to identifying the active site of the SWI/SNF ATPase, the locations of the different polypeptides within the 3D volume and the nucleosome interaction site(s).

Note added in proof: During review of this manuscript, a 3D reconstruction of the RSC chromatin remodeling complex was published¹⁸ that similarly describes a putative nucleosome-binding site in a cavity surrounded by a ring of protein densities.

Methods

Tagged SWI2 strains and immunoprecipitations. Whole cell extracts were made from isogenic W303 yeast strains encoding an HA-tagged SWI2 at the *URA3* locus (CY831), an Myc₁₈-tagged SWI2 at the endogenous locus (CY832) or by combining both the HA₃- and Myc₁₈-tagged SWI2 epitopes (CY889). Immunoprecipitations were conducted as reported⁴ and binding was analyzed by SDS-PAGE and western blot analysis with anti-HA (HA.11; Babco) or anti-Myc (9E10; Santa Cruz Biotechnology). Western blots were visualized using enhanced chemiluminescence (ECL) reagents (Lumiglo; KPL).

SWI/SNF purification. SWI2 was C-terminally tagged in frame at the endogenous locus with a calmodulin–protein A TAP tag as described⁸. Cultures were grown in YPD with 2% (w/v) glucose until OD₆₀₀ = 2.0. Cells were harvested and lysed by mechanical bead lysis in buffer E (20 mM HEPES, pH 7.4, 350 mM NaCl, 10% (v/v) glycerol and 0.1% (v/v) TWEEN and protease inhibitors (1 mM PMSF, 2 μg ml⁻¹ pepstatin and 2 μg ml⁻¹ leupeptin). Lysates were clarified at 40,000g at 4 °C for 45 min (Ti45 Beckman rotor). Cleared lysates were incubated with IgG-Agarose (Sigma), eluted by TEV protease cleavage and incubated with calmodulin affinity resin (Stratagene) in buffer E plus 2 mM CaCl₂. Purified complex was eluted from calmodulin resin in buffer E plus 10 mM EGTA. Samples were then concentrated and dialyzed against buffer E with 50 μM ZnCl₂. Purity was verified by silver staining.

Stoichiometry determination of SWI/SNF. Purified TAP-SWI/SNF was denatured by the addition of SDS and labeled with [¹²⁵I]NaI in the presence of chloramine T⁶. Labeling was quenched with Na₂S₂O₅. Labeled material was precipitated with potassium acetate on ice for 30 min and diluted in protein sample buffer. Labeled SWI/SNF was loaded on SDS-PAGE gels and ran at constant voltage. After electrophoresis, gels were fixed and washed in 10% (v/v) acetic acid and 40% (v/v) methanol for ~20 h. Gels were dried and then imaged, and densitometry was performed using a PhosphorImager (Molecular Dynamics). Radio-iodinations were performed several times, and each labeling was fractionated on multiple SDS-PAGE gels. The amount of radioactivity present within the gel wells was variable among different gels (Fig. 2), and the calculated subunit stoichiometries were independent of such signals.

STEM. For accurate STEM mass measurements, salts and other buffer components must be removed from the samples. This was achieved by crosslinking TAP-purified SWI/SNF at ~100 nM in buffer E by direct addition of 0.1% (v/v) glutaraldehyde for 4 h, followed by dialysis against 50 mM NaCl, 10 mM HEPES, pH 7.4, and 0.2 mM EDTA, or by dialyzing overnight against buffer E containing 0.1% (v/v) glutar-

aldehyde without glycerol, zinc or TWEEN, then against the lower salt 50 mM NaCl buffer. Both methods resulted in stable SWI/SNF complexes, with no significant difference in mean mass. Freeze dried specimens were prepared by the wet film method^{9,14} and imaged at the Brookhaven National Laboratory STEM Facility. A 2 μl sample of 100 μg ml⁻¹ tobacco mosaic virus (TMV), an internal mass standard, were adsorbed for 1 min onto freshly prepared carbon films supported by a holey film on a titanium grid (Ernest F. Fullam, Inc.). After washing the grid 4×, 3 μl of fixed SWI/SNF solution was applied by injection into the droplet on the grid. The grid was allowed to adsorb for 1 min and then rinsed 4× with sample buffer, followed by rinses of 100 mM ammonium acetate (~5×) and 20 mM ammonium acetate (~5×) to remove nonvolatile salts. After the final wash, the grid was blotted between two pieces of filter paper, leaving a retained layer <1 μm thick, and immediately plunged into liquid nitrogen slush. The frozen samples were transferred to an ion-pumped chamber and freeze dried overnight by gradually warming to -80 °C. They were then transferred under vacuum to the STEM. Specimens were imaged in the STEM at 40 kV with a probe focused to 0.25 nm. Focusing was at a high magnification near the area of interest and the data acquired on the first scan. The average dose of electrons for the single scan to record the data was <1,000 e⁻ nm⁻², assuring that the mass loss from radiation damage was not >2% at the -150 °C specimen temperature⁹. Digital images were recorded from large and small angle detectors for unstained specimens. In images used for mass measurements, the pixels were separated by 1 nm, giving a scan width of 0.512 μm. The masses of selected particles were determined using the program PCMass23 (ref. 15). This program sums the number of scattered electrons over a defined area bounding the particle, subtracts a background obtained from areas not containing particles and multiplies the result by a standard STEM calibration constant (115 Da / e⁻ with 1 nm pixels) to determine the mass. Further data analysis and histogram generation used PSI Plot (Polysoftware International).

Electron microscopy and 3D image reconstruction.

Crosslinked SWI/SNF was adsorbed to glow-discharge carbon films, negatively stained with 1.5% (w/v) sodium phosphotungstate, pH 7.2, containing 0.015% (w/v) glucose¹⁶, and observed with a Tecnai 12 electron microscope (FEI Inc.) at 80 kV. Digital images were recorded at 800 nm defocus with a cooled 2,048 × 2,048 CCD camera (TVIPS GmbH) and a pixel size of 6.32 Å. Data sets for reconstruction contained 5,000–10,000 images free of astigmatism and drift. Examination of the data sets showed that there was no preferential orientation of SWI/SNF on the carbon film.

Single particle reconstruction was carried out with EMAN¹¹ (ncmi.bcm.tmc.edu/homes/steve/EMAN/doc). First, an initial model was generated by reference-free classification. This starting model was then used to begin an iterative refinement of the classification. Convergence was judged by the absence of change in the Fourier shell correlation (FSC) of subsequent iterations¹¹. The resolution of each reconstruction was estimated using the FSC of two semi-independent reconstructions derived by dividing the data in the final class averages in half¹⁷. FSC was also used to evaluate the similarity of the three different reconstructions, using the 0.5 value as the limit of congruence. Volumes were constrained to a mass of 1.14 MDa, assuming a protein density of 1.35 g ml⁻¹ (0.81 Da Å⁻³), and gaussian low-pass filtered to the 0.5 FSC threshold. Data processing and visualization with AVS (AVS Inc.) and VIS5D (<http://vis5d.sourceforge.net>) was performed on a multiprocessor Silicon Graphics Octane (SGI Inc.).

Acknowledgments

We thank B. Cairns for communicating the unpublished sequence of SWP82, D. Kelleher for help with the radio-iodination studies, S.J. Ludtke for assistance with EMAN and J.S. Wall and M. Simon of the Brookhaven National Laboratory STEM Facility for mass determination. The STEM is an NIH Research Resource also supported by DOE and OBER. These studies were supported by NIH grants to C.L.W. and to C.L.P.

Competing interests statement

The authors declare that they have no competing financial interests.

Received 28 August, 2002; accepted 10 December, 2002.

- Peterson, C.L., & Tamkun, J.W. The SWI-SNF complex: a chromatin remodeling machine? *Trends Biochem. Sci.* **20**, 143–146 (1995).
- Fry, C.J., & Peterson, C.L. Chromatin remodeling enzymes: who's on first? *Curr. Biol.* **11**, R185–R197 (2001).
- Vignali, M., Hassan, A.H., Neely, K.E., & Workman, J.L. ATP-dependent chromatin-remodeling complexes. *Mol. Cell. Biol.* **20**, 1899–1910 (2000).
- Côté, J., Quinn, J., Workman, J., & Peterson, C. L. Stimulation of GAL4 derivative binding to nucleosomal DNA by the yeast SWI/SNF complex. *Science* **265**, 53–60 (1994).
- Kwon, H., Imbalzano, A.N., Khavari, P.A., Kingston, R.E., & Green, M.R. Nucleosome disruption and enhancement of activator binding by a human SWI/SNF complex. *Nature* **370**, 477–481 (1994).
- Kelleher, D.J., & Gilmore, R. DAD1, the defender against apoptotic cell death, is a subunit of the mammalian oligosaccharyltransferase. *Proc. Natl. Acad. Sci. USA* **94**, 4994–4999 (1997).
- Rigaut, G. et al. A generic protein purification method for protein complex characterization and proteome exploration. *Nat. Biotechnol.* **17**, 1030–1032 (1999).
- Tasto, J.J., Carnahan, R.H., McDonald, W.H., & Gould, K.L. Vectors and gene targeting modules for tandem affinity purification in *Schizosaccharomyces pombe*. *Yeast* **18**, 657–662 (2001).
- Wall, J.S., Hainfeld, J.F. & Simon, M. Scanning transmission electron microscopy of nuclear structures. *Methods Cell Biol.* **53**, 139–164 (1998).
- Schnitzler, G.R. et al. Direct imaging of human SWI/SNF-remodeled mono- and polynucleosomes by atomic force microscopy employing carbon nanotube tips. *Mol. Cell. Biol.* **21**, 8504–8511 (2001).
- Ludtke, S.J., Baldwin, P.R., & Chiu, W.J. EMAN: semiautomated software for high-resolution single-particle reconstructions. *J. Struct. Biol.* **128**, 82–97 (1999).
- Luger, K., Mader, A.W., Richmond, R.K., Sargent, D.F., & Richmond, T.J. Crystal structure of the nucleosome core particle at 2.8 Å resolution. *Nature* **389**, 251–260 (1997).
- Bazett-Jones, D.P., Côté, J., Landel, C.C., Peterson, C.L. & Workman, J.L. The SWI/SNF complex creates loop domains in DNA and polynucleosome arrays and can disrupt DNA-histone contacts within these domains. *Mol. Cell. Biol.* **19**, 1470–1478 (1999).
- Wall, J.S. & Hainfeld, J.F. Mass mapping with the scanning transmission electron microscope. *Ann. Rev. Biophys. Biophys. Chem.* **15**, 355–376 (1986).
- Hainfeld, J.F., Wall, J.S. & Desmond, E.J. A small computer system for micrograph analysis. *Ultramicroscopy* **8**, 263–270 (1982).
- Woodcock, C.L., Woodcock, H., & Horowitz, R.A. Ultrastructure of chromatin. I. Negative staining of isolated fibers. *J. Cell Sci.* **99**, 99–106 (1991).
- Serysheva, I.I., Schatz, M., van Heel, M., Chiu, W., & Hamilton, S.L. Structure of the skeletal muscle calcium release channel activated with Ca²⁺ and AMP-PCP. *Biophys. J.* **77**, 1936–1944 (1999).
- Asturias, F.J., Chung, W.H., Kornberg, R.D. & Lorch, Y. Structural analysis of the RSC chromatin-remodeling complex. *Proc. Natl. Acad. Sci. USA* **99**, 13477–13480 (2002).